Radar Sea Returns—Ocean-Ripple Spectrum and Breaking-Wave Influence

JIN WU

Air–Sea Interaction Laboratory, College of Marine Studies, University of Delaware, Lewes, Delaware

27 December 1989 and 5 July 1990

ABSTRACT

Radar cross sections reported by Guinard et al. are normalized with respect to their mean value obtained with different bands but at the same wind velocity. The results confirm that there are significant differences between returns with VV and HH polarizations. The VV-polarized returns, being associated more closely with distributed ocean ripples, support the equilibrium spectrum of ocean waves $k^{-3.5}$ with the wavenumber $k < 0.5$ rad cm^{-1}, and the saturated spectrum k^{-4} at higher wavenumbers. The HH-polarized returns at low wavenumbers have the same trend as those of the VV-returns, but are smaller in magnitude. At high wavenumbers ($k > 0.5$ rad cm^{-1}), the HH-returns retain the trend of increasing continuously with the Bragg wavenumber; this is believed to be caused by the surface roughness produced by individual breaking waves. Contributions of returns produced by each mechanism are then discussed for radars having various bands. Functional, power-law type, dependence of returns on the wind-friction velocity is also found to vary systematically with the Bragg wavenumber; the exponent of power law increases with the Bragg wavenumber, following $k^{1/3}$.

1. Introduction

Many types of sensors have been promoted for the remote sensing of oceanic parameters. Among them, the scatterometer operated on the Bragg scattering mechanism has provided the most excitement as a prospective means of mapping sea-surface winds (Moore and Fung 1979). Following many demonstrations of its feasibility, Phillips (1988) took a critical look at the sea-surface features that serve as Bragg scatterers and attempted to relate the radar returns mostly to ocean ripples; these are short gravity waves and capillary waves well distributed over the sea surface. He proposed a scaling parameter, grouped from the radar wavenumber, wind-friction velocity and gravitational acceleration, for returns with both vertical–vertical (VV) and horizontal–horizontal (HH) polarizations. The same group of data used by Phillips (1988) are herewith analyzed to evaluate separately dependences of the returns on the radar wavenumber and on the wind velocity. The difference is shown to exist between radar cross sections obtained with VV and HH polarizations, as summarized in Woiceshyn et al. (1986); the results are most revealing to studies of ocean-ripple structures and remote sensing, as advocated by Phillips (1988). The spectrum of short gravity waves is again confirmed to reach an equilibrium state (Phillips 1985), following the dropoff of $k^{-3.5}$ with wavenumbers up to about 0.5 rad cm^{-1}. However, the spectrum of shorter waves, consisting of shortest gravity waves and waves in the gravity–capillary region, does reach a saturated state as indicated by the k^{-4} shape (Phillips 1958). Surface roughnesses produced by individual breaking waves are shown to be closely associated with the HH-polarized returns; but this occurs only at high wavenumbers (>0.5 rad cm^{-1}). These roughnesses can be detected by only X and C bands or shorter wavelength radars. Relative contributions of ocean ripples and breaking waves to radar sea returns at these bands are also discussed. Finally, the exponent of the power law relating the return to wind velocity is shown to increase, as the Bragg wavenumber increases.

2. Bragg scattering from the sea surface

a. Radar returns and Phillips' scaling

Phillips (1988) considered that radar returns from the sea surface consisted of two different types of Bragg scatterers: ocean ripples and surface roughnesses produced by breaking waves. The following expression was proposed,

$$\sigma_0 = \frac{\pi B}{2\sqrt{2}} |\cos\phi|^{1/2} \sin^{1/2}\theta \cot^4\theta F_1(\theta)\left(\frac{u_*^2\kappa}{g}\right)^{1/2} + F_2(\theta, \phi)\left(\frac{u_*^2\kappa}{g}\right)^{3/2} \quad (1)$$

where σ_0 is the radar cross section, B is the coefficient of ocean-wave spectrum in the equilibrium range, θ is the incidence angle of the radar beam with respect to the mean sea surface, ϕ is the observational direction

Corresponding author address: Prof. Jin Wu, University of Delaware, Air–Sea Interaction Laboratory, College of Marine Studies, Lewes, DE 19958.

with respect to the wind, u_* is the wind-friction velocity, κ is the radar wavenumber, g is the gravitational acceleration, and $F_1(\theta)$ and $F_2(\theta)$ are coefficients depending on the polarization of transmitted and received microwave signals. The first term on the right side of the above expression is associated with distributed ripples, and the second term with individual breakers.

Phillips' (1988) major theme is that radar returns from both ripples and breakers can be scaled with the dimensionless parameter $u_*^2\kappa/g$. The dependence of these two kinds of returns on the proposed parameter, however, differs; see Eq. (1). The returns from ripples are shown to be proportional to $(u_*^2\kappa/g)^{1/2}$. This was suggested to be consistent with the spectrum for short gravity waves in the equilibrium range revised recently by Phillips (1985),

$$\psi(\mathbf{k}) = B|\cos\phi|^{1/2}u_* g^{-1/2}k^{-7/2} \qquad (2)$$

where $\mathbf{k}$ and k are wavenumber vector and scalar of surface waves, respectively. According to the Bragg scattering mechanism, the radar and Bragg wavenumbers are related through

$$k = 2\kappa \sin\theta \qquad (3)$$

As the wavelength of radars is generally short, their returns are mostly associated with ocean ripples, best described by the slope statistics (Valenzuela 1978). The wavenumber slope spectrum corresponding to the elevation spectrum shown in Eq. (2) has the form of $S(\mathbf{k}) \sim k^{1/2}$, being proportional approximately to $\kappa^{1/2}$. These, therefore, explain the dependency of returns on the radar wavenumber as $\kappa^{1/2}$ (Phillips 1988).

The sea returns were measured by Guinard et al. (1971) simultaneously with radars of X, C, L and P bands. Wavelengths of these bands are X: 3.4 cm, C: 6.9 cm, L: 24 cm and P: 70 cm. Guinard et al.'s results were used by Phillips (1988) to substantiate the scaling of radar returns with his proposed parameter, $(u_*^2\kappa/g)^{1/2}$. His consideration of all returns following roughly this scaling implies that they are primarily from ocean ripples, instead of surface roughnesses produced by breaking waves. For the latter, the scaling as shown in Eq. (1) was suggested to be with $(u_*^2\kappa/g)^{3/2}$. There are also other physical implications; the returns are not only similar with both polarizations, but also have similar functional dependences on the wind-friction velocity for all radar wavenumbers.

b. *Radar backscattering and sea-surface roughness*

1) A PRELIMINARY LOOK

According to the scaling of $(u_*^2\kappa/g)^{1/2}$ and therefore of $\kappa^{1/2}$ under the same wind velocity, the magnitude of returns at the same incidence angle from large to small should be provided in order by X, C, L and P bands. We have compiled in Table 1 the actual order of returns observed by Guinard et al. (1971) and shown in Fig. 2 of Phillips (1988). In the table, the results obtained with two polarizations at different incidence angles are separately tabulated; the trends, at each incidence angle, are generally consistent for all wind velocities.

TABLE 1. Orders in the magnitude of radar sea returns observed by Guinard et al. (1971) under the same wind velocity but from different bands. For both polarizations, the magnitude of returns at each incidence angle decreases from left to right, and the trends are consistent for all wind velocities.

Incidence angle θ (deg)	Vertical–vertical polarizations	Horizontal–horizontal polarizations
30	L C X P	X L C P
45	L C X P	X L C P
60	L C X P	X C L P
70	L C X P	X C L P
80	C L X P	X C L P
85	C L X P	X C L P

As illustrated in Table 1, the returns with HH polarization follow mostly the Phillips' (1988) suggestion, in the decreasing order of X, C, L and P bands. Those with VV polarizations, however, are very much out of the suggested order. These surprising trends are important, since Guinard et al.'s (1971) data, as mentioned previously, were used by Phillips to illustrate the $(u_*^2\kappa/g)^{1/2}$ scaling, as well as to confirm the recently revised spectrum of ocean waves (Phillips 1985). The discrepancy is especially critical, as VV-polarized returns are believed to be associated more closely with the Bragg scattering from ocean ripples, and the horizontally polarized returns, on the other hand, are more influenced by isolated features (Duncan et al. 1974). Subsequent studies indicated that these features might be associated with breaking waves (Banner and Fooks 1985). The trends shown in Table 1, therefore, have great implications on not only radar returns but also structures of ocean waves, motivating us to take a closer look. In addition, recent measurements of Banner et al. (1989), to be discussed later, also departed from Phillips' (1985) equilibrium spectrum at high wavenumbers.

2) A CLOSER LOOK

With simultaneous observations of four bands, the study of Guinard et al. (1971) was designed primarily for investigating the dependence of radar returns on its wavelength. The wind velocity was not their principal concern, and therefore might not be very accurately measured by them. Thinking along this line, the wind-friction velocity was only roughly estimated by Phillips (1988). Moreover, there are many other studies designed especially for evaluating the dependence of radar returns on the wind velocity (Woiceshyn et al. 1986; Masuko et al. 1986). We, therefore, concentrate first on exploring further the primary results obtained in Guinard et al.'s investigation; following Phillips

(1988), only the data from the upwind look are used. For each wind condition, the returns from four bands are averaged to obtain $\bar{\sigma}_0$; subsequently, the power ratio between the actual and averaged returns for a given band, $\sigma_0/\bar{\sigma}_0$, is determined. Through this normalization, the variation of the radar returns with the wind velocity is removed to retain only that with the wavelength of Bragg scatterers. The results at various incidence angles are presented versus the wavenumber of corresponding Bragg scatterers in Fig. 1. For the clarity of the presentations, we did not include the data at the lowest wind velocity of 2.5 m s^{-1}. The results at this

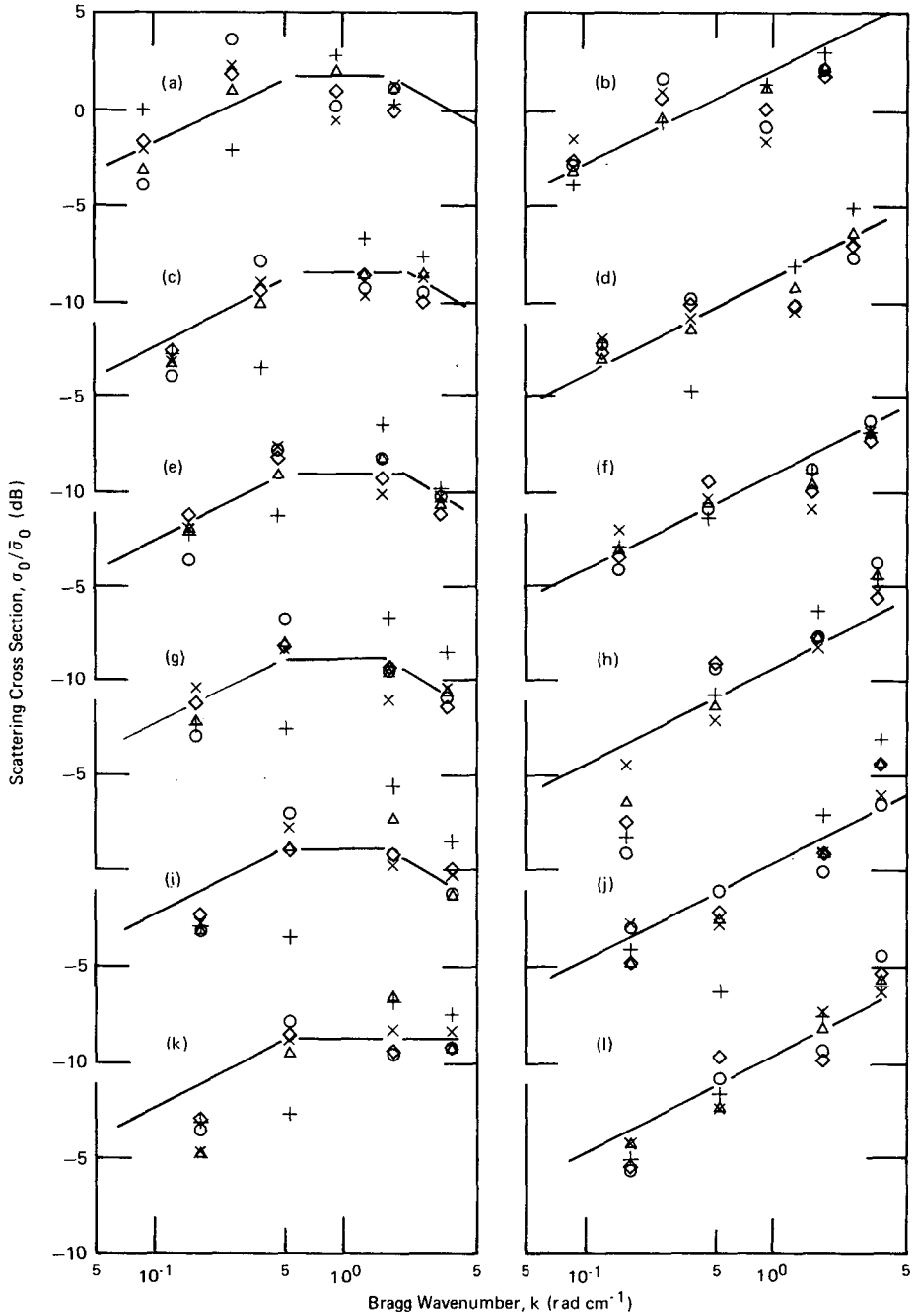

FIG. 1. Variation of radar return with surface-wave number. The data were obtained by Guinard et al. (1971) at five wind velocities. The left column was obtained under VV polarizations and the right under HH polarizations; in each column from top to bottom the data were obtained at incident angles of 30, 45, 60, 70, 80 and 85°; and various symbols are for different wind velocities (m s^{-1}): 11.3 (×), 16.2 (+), 19.0 (◇), 20.6 (△) and 24.2 (○).

wind velocity, which separates distinctly from the others, follow the same trend but are more scattered.

Lines are drawn in Fig. 1 to approximate trends of the data; more on the fitted line will be discussed in a later section. It is shown that there is a distinct difference, in both trends and magnitudes, between VV and HH returns. The HH returns increase continuously with the wavenumber; the VV returns follow such a trend only at low wavenumbers, and reach a saturated shape, being invariant with the wavenumber, at high wavenumbers. Phillips (1988) noticed that there was a hint of saturation at large values of $(u_*^2\kappa/g)^{1/2}$; the saturation is clearly displayed here but with only VV returns. At low wavenumbers where both HH and VV returns have the same trend, HH returns are smaller in magnitude; the latter was also noted in Woiceshyn et al. (1986). All these suggest that returns with HH and VV polarizations are probably governed by different mechanisms. Consequently, we must analyze separately these two types of returns and must examine them with respect to different mechanisms.

Note that the data reported by Guinard et al. (1971) were tabulated in Daley et al. (1970). Following Phillips (1988), only the data from the upwind look are used in Fig. 1 for the convenience of a direct comparison with results and interpretations reported in that paper. We, however, have analyzed in a similar fashion the data averaged from upwind and downwind looks; the results have identical trends as those shown in Fig. 1.

3. Mechanisms governing radar sea returns

a. VV-polarized returns and wave spectrum

As discussed previously, the radar returns with VV polarizations are known to be associated closely with the spectrum of ocean ripples (Phillips 1988). The return should be proportional with the spectral density of Bragg scatterers, of which the most commonly encountered as discussed earlier are short in length. On the other hand, measurements of ocean waves have been limited generally to rather long components. Therefore, we can benefit from results of the observed Bragg scatterers in studying the spectrum of short gravity waves and even capillary waves. This idea, of course, was originated and advanced by Phillips (1985, 1988).

1) EQUILIBRIUM REGION

The portion of the spectrum in the range of frequencies extending from that at the spectral peak to that about triple the peak frequency is in the so-called equilibrium range (Phillips 1985), within which the spectral density is limited dynamically by wave breaking. This portion of the spectrum has been widely studied and generally considered to have the form of $\psi(\mathbf{k}) \sim k^{-3.5}$ (Phillips 1985). Correspondingly, the spectral density expressed in terms of the surface slope follows $S(\mathbf{k}) \sim k^{0.5}$, as mentioned previously. This is illustrated by lines drawn to approximate the returns at low wavenumbers shown in Fig. 1. The region to which this spectrum is applicable was previously unknown, but can be determined here as up to the wavenumber of about 0.5 rad cm^{-1}. This is well within the gravity region, as the dividing wavenumber for the capillary and gravity ranges is about 3.63 rad cm^{-1}. The equilibrium spectrum is also sketched in Fig. 2a.

2) SATURATION REGION

The spectrum of gravity waves was first proposed by Phillips (1958) to be saturated at high wavenumbers, where the spectral density was invariant with either the wavenumber or the wind velocity. The height and slope spectra in the saturation range were thought to follow $\psi(k) \sim k^{-4}$ and $S(\mathbf{k}) \sim k^0$, respectively. Subsequent studies (Longuet-Higgins 1969; Liu 1971; Hasselmann et al. 1973; Kitaigorodskii 1983; Donelan et al. 1985) suggested that the spectral density might be invariant with the wavenumber at certain wind and fetch conditions, but not universal. Finally, this long-standing concept was considered to be no longer attainable (Phillips 1985). There are two major reasons which have pushed for this revision; measurements of rela-

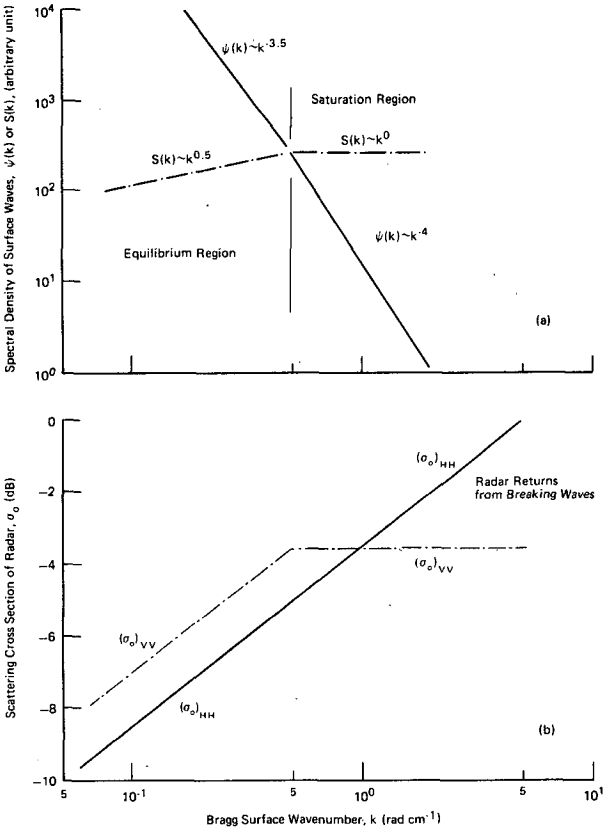

FIG. 2. Shapes of surface-wave spectra (a) and features of radar sea-returns (b).

tively long waves have shown to consist of only the equilibrium range, and contradictory evidence has been suggested to be provided by microwave sea returns from ocean ripples.

The situation is further clarified here. While the saturation region as indicated by the spectrum does exist, it is at wavenumbers much higher than those suggested originally by Phillips (1958). These are illustrated by the results shown in Fig. 1, especially those obtained at incidence angles of 30°, 45° and 60°; the Bragg mechanism may not be fully operable at larger incidence angles. The saturation spectrum is now seen to be in the region, 0.5 rad $cm^{-1} < k < 5$ rad cm^{-1}. This appears to be consistent in concept with recent results of stereophotography reported by Banner et al. (1989) that the k^{-4} wave spectrum does exist at high wavenumbers. Quantitatively, however, their results show that the spectrum is saturated in the region of 0.04 rad $cm^{-1} < k < 0.3$ rad cm^{-1} are not substantiated by the radar results presented here. In fact, the present results support Phillips' (1988) assertion that the equilibrium range prevails for gravity wave components while the saturation range exists only for shortest-gravity and gravity–capillary wave components. Note that in situ measurements of waves cited by Phillips (1985) in establishing the equilibrium spectrum were limited to components no shorter than say a meter; these are much longer than those discussed in this article, especially that in the saturation range.

We are concerned mostly here with the wave spectrum shape. It will be shown later that the Bragg scattering from the wavenumber region of 0.5–5 rad cm^{-1} still has a wind-velocity dependence. Such a dependence, although a weak one, was also reported by Banner et al. (1989). Much of these will be left to be resolved by future direct wave and refined wind measurements.

3) Capillary region

The spectrum in the capillary range has not been extensively studied; a probable sharp dropoff of the spectral density within this region was discussed in Phillips (1977). Signs of such a dropoff can be seen from VV returns in Fig. 1 at incidence angles of 30°, 45° and 60°. Again, the results at these angles are most closely associated with the structure of ripples. Short lines are drawn in the figure to show that those three returns can be approximated with the forms of $\psi(\mathbf{k}) \sim k^{-4.5}$ and $S(\mathbf{k}) \sim k^{-0.5}$.

b. HH-polarized returns and breaking waves

The ratio between HH and VV polarized returns with an X-band radar was found by Duncan et al. (1974) to be generally smaller than unity at low winds, and increase toward unity at high winds. Such an increase of HH returns at high winds was associated by them, and also later by Lee (1977), with those scatterers moving at or near the phase velocity of dominant waves. Subsequently, experiments were conducted by Banner and Fooks (1985), also with an X-band radar, to confirm that this portion of returns is consistent with Bragg scattering from the surface roughnesses produced by breaking waves. Mechanisms causing sea spikes, however, are not entirely clear at this stage, specular reflection and wedge diffraction could also be important (Kwoh et al. 1988); both effects are, nonetheless, related to breaking waves. With this understanding in mind, let us examine more closely the spectrally resolved results in Fig. 1.

1) Spectral response

The pattern of returns displayed by the results shown in Fig. 1 is sketched in Fig. 2b. At low wavenumbers, the HH-returns being similar to the above findings are proportionally smaller than the VV-returns. The HH returns are about 1.9 dB less than VV returns at incidence angles of 30°, 45° and 60°, and by about 1.3 dB at larger incidence angles of 70° and 80°. At higher wavenumbers ($k > 0.5$ rad cm^{-1}), the portion of HH-returns, identified above to be closely associated with breaking waves, continues to increase with the wavenumber. Consequently, we find that the returns from breaking waves can be better detected with radars of X and C bands or those having shorter wavelengths. The wavelengths of L and P bands are too long, where less scatterers locked in phase with breaking waves can be effectively detected.

2) Relative contributions

Earlier, the radar returns were associated exclusively with ocean ripples; recently, effects of breaking waves were noted. In both cases, the returns were interpreted by only one mechanism, while undoubtedly both mechanisms contribute simultaneously to the returns. Referring to the illustration in Fig. 2b and the results in Fig. 1, we see that the returns at low wavenumbers are primarily from ocean ripples, and those at high wavenumbers are from surface roughnesses produced by breaking waves. Needless to say, much more still needs to be studied to quantify these partitions, the present results serve to identify the wavelength region of dominance of each scattering mechanism. Note that under high winds, the sea-surface wind velocity deduced from HH-returns from a K-band radar (2.05-cm wavelength) was found by Wentz et al. (1986) to be about 5 m s^{-1} greater than that deduced from VV-returns. The present results, while in about the same magnitude, indicate that the difference also depends on the wavelength of Bragg scatterers.

4. Parameterization of radar sea returns

a. Dependence of radar returns on wind-friction velocity

1) Two limits

In the last section, we have identified the mechanisms governing sea returns of radars having various

wavelengths. The returns from radars having longer lengths of L and P bands are shown to be mostly associated with ocean ripples, and those from shorter-length bands are with both ocean ripples and surface roughnesses produced by breaking waves. Having discussed the dependence of radar returns on its wavelength, we now take a look at their dependence on the wind-friction velocity. The power-law type dependence shown in Eq. (1) has been generally accepted; it has provided the basis of scatterometer algorithm (Jones and Schroeder 1978; Schroeder et al. 1982; Woiceshyn et al. 1986). The linear dependence of the spectral density of ocean ripples in the equilibrium range on the wind-friction velocity has also been rigorously argued by Phillips (1985). For returns from ocean ripples in the equilibrium range, the exponent of unity on their dependence of the wind-friction velocity in the form of $\sigma_0 \sim u_*$ can be considered as the lower limit. The dependence associated with breaking waves shown as $\sigma_0 \sim u_*^3$ in Eq. (1) is confirmed by recent microwave observations (Jessup et al. 1990); it is also consistent with results on the sea-surface whitecap coverage (Wu 1988). This latter exponent can be considered as the upper limit. We, therefore, believe that the exponent of power law should vary between these two limits, depending on the radar wavelength and its operating incidence angle.

2) GUINARD ET AL.'S RESULTS

We have discussed earlier that Guinard et al.'s (1971) study was primarily for evaluating radar returns on its wavelength. Our discussion in the last section concentrated indeed on this regard; their data are shown to be very helpful in studying the scattering mechanisms as well as the ocean-wave spectrum. We now attempt to see whether their data can also be used to resolve the dependency of radar returns on the wind-friction velocity. The wind-stress coefficient suggested by Wu (1980) is used to calculate the wind-friction velocity. The data obtained at incidence angles of 30°, 45° and 60° are used, as those at 70° and 80° are either on the border line of, or outside, the region within which the Bragg scattering is operable (Valenzuela 1978). The results obtained at each band with two polarizations, VV and HH, are shown in Figs. 3 and 4. Additional data from two more wind velocities, 14.9 and 20.6 m s^{-1}, were obtained from Daley et al. (1970) and added here.

As discussed previously, the experiments of Guinard et al. (1971) were not directed at studying the variation of microwave returns with the wind velocity. The experimental conditions are, as seen in Figs. 3 and 4, not well distributed over the range of wind velocities covered. An overall inspection of the results in these two figures shows, nonetheless, that the variation of radar returns with the wind-friction velocity is distinctly different at various radar wavelengths. The variation of returns with the wind-friction velocity becomes more gradual, as the radar wavelength increases. A line representing the power-law variation is fitted to approximate the trend of each set of data. We then see little differences between results obtained at incidence angles of 30° and 45°, while the results obtained at the incidence angle of 60° are significantly different. This suggests that the Bragg scattering may operate at a narrower region than previously suggested up to about 70°. The slope of the fitted line, corresponding to the exponent of the power law obtained from Figs. 3 and 4, is presented in Fig. 5. In this figure, the major portion of exponents obtained from Guinard et al.'s (1971) results is seen to be below the lower limit of unity. More studies are needed to understand these small values of the exponent shown in the figure. Nonetheless, these exponents are seen clearly to decrease systematically as the radar wavelength increases.

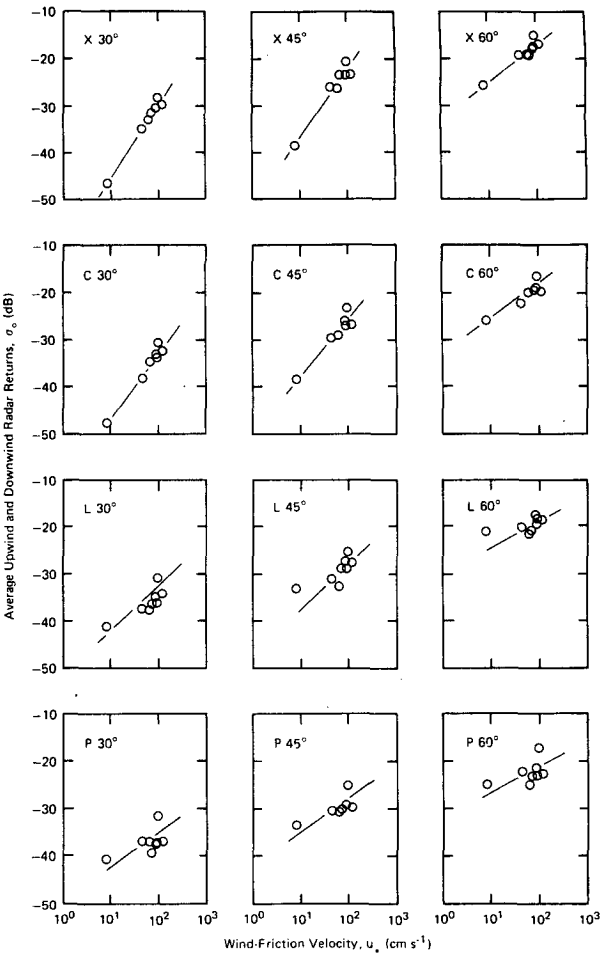

FIG. 3. Horizontally polarized radar returns obtained with different bands under various winds. The radar data are from Guinard et al. (1971).

3) GENERAL RESULTS

Data from measurements of microwave backscattering signatures of the ocean surface (Jones and Schroeder 1978; Moore and Fung 1979; Fung and Lee 1982; Schroeder et al. 1982; Schroeder et al. 1984; Feindt et al. 1985) were all expressed in the power-law form in terms of the wind velocity, $\sigma_0 \sim U^n$. The wind velocity was measured at different elevations by these investigators. Reported results on the exponent n were compiled by Masuko et al. (1986) along with those of their own. Inasmuch as we intend only to examine a general trend rather than quantitative variation of the exponent, we consider for this portion of the data, as in Phillips (1988), that the wind-stress coefficient does not vary with the wind velocity. Therefore, the exponent with the results expressed in terms of the wind-friction velocity is the same as that in terms of the wind velocity.

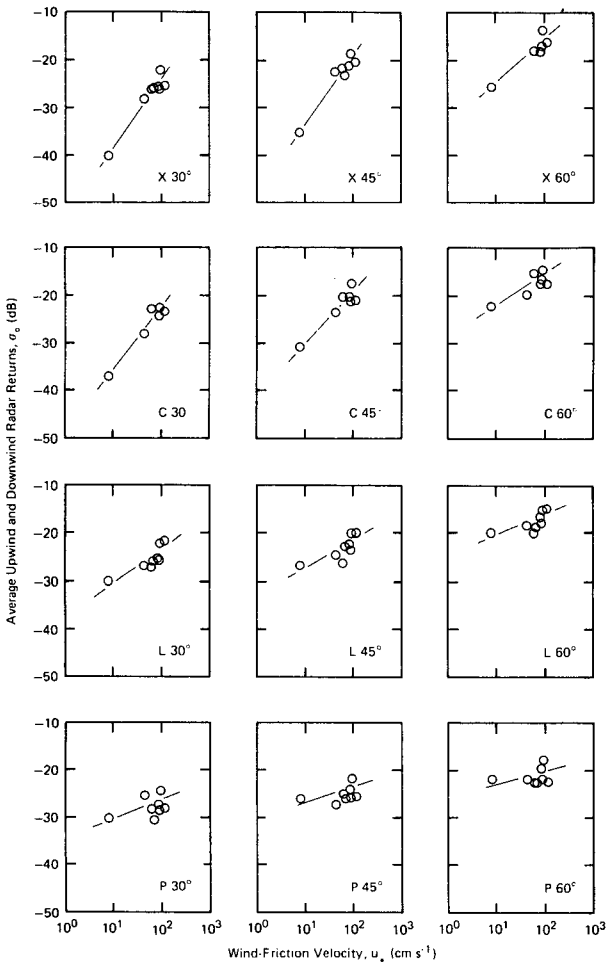

FIG. 4. Vertically polarized radar returns obtained with different bands under various winds. The radar data are from Guinard et al. (1971).

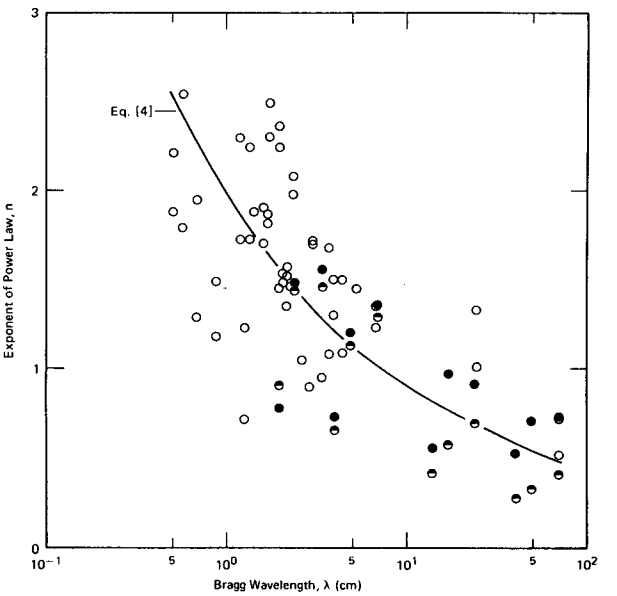

FIG. 5. Variation of power-law exponent with Bragg wavelength. The data obtained in various investigations and compiled by Masuko et al. (1986) are shown as open symbols; those from Figs. 3 and 4 are shown respectively as solid and half-solid symbols.

The results compiled by Masuko et al. on the exponent were obtained over the range of radar wavelengths of 0.87–70.1 cm, and at incidence angles of 20°–60°. In order to evaluate the functional variation of these results, the corresponding Bragg wavelengths for the data are calculated; the final results are presented in Fig. 5, where λ is the Bragg wavelength. The trend is now quite clear; the exponent decreases as the Bragg wavelength increases. The data appear to follow the mean line drawn in the figure,

$$n = 2\lambda^{-1/3} \tag{4}$$

where λ is expressed in cm. The above expression is intended to illustrate only a general trend that the exponent varies systematically with the Bragg wavelength. As pointed out by Phillips (1988), there are problems involved in the instrument calibration and data averaging in some of the studies from which the results are shown in Fig. 5. Furthermore, the scattering of results can also be caused by various environmental factors; the latter includes wind stress and atmospheric stability (Keller et al. 1985).

4) SUMMARY

Consistent results from all available studies are illustrated in Fig. 5; the power-law dependence of radar returns on the wind-friction velocity varies with the Bragg wavelength. In other words, the exponent of power law varies with not only radar bands as suggested

by Donelan and Pierson (1987) but also with its incidence angles. This, of course, differs from the linear dependence for all radar bands shown in Eq. (1). Much of the suppressed variation of the dependence of radar returns on the wind-friction velocity discussed in Phillips (1988) appears to be caused by fitting a straight line to the entire group of Guinard et al.'s (1971) data. The returns, especially those with VV-polarization shown in Table 1, do not follow a linear increase with the scaling parameter $(u_*^2\kappa/g)^{1/2}$.

b. *Parameterizations of radar returns for different regions*

Before discussing the parameterization of returns at various radar wavelengths, we need to explain the trend shown in Table 1. For longer-wavelength bands, the HH returns follow the expected trend, with the P band providing a greater return than the L band. As for the returns from C and X bands, they are also approximately in order, as the spectral density of ripples start to drop off for the wavenumber region covered by the X band.

The very bases of the parameterization proposed by Phillips (1988) are that the spectrum of surface waves follows a universal shape of $\psi(\mathbf{k}) \sim k^{-3.5}$, and that the radar returns from all bands increase linearly with the wind-friction velocity, $\sigma_0 \sim u_*$. We show here that both of these cannot be generally scaled. While the returns from L and P bands and radars of longer wavelengths are from the same equilibrium range, those from X and C bands and shorter wave lengths are from the saturation range. In other words, the $k^{1/2}$-scaling is still applicable to longer-wavelength cases; the k^0-scaling is needed for shorter-wavelength cases. As for the linear relationship between the radar return and wind-friction velocity, it appears to under-represent the shorter-wavelength cases of X and C bands, and over-represent the longer-wavelength cases of L and P bands. A general power law of parameterizing the radar returns may not be attainable as discussed earlier by Donelan and Pierson (1987), and illustrated quite clearly in Fig. 5.

5. Concluding remarks

Much has been demonstrated on the feasibility of using radar Bragg scattering for measuring sea-surface winds. Sets of field data have already been compiled, along with many empirical correlations. For further advances, we need to examine in more details the available data to explore deeper the mechanism of backscattering. Needless to say, those radar returns can also help us to understand surface-wave dynamic; such as what Phillips (1988) did earlier and we are doing here.

Acknowledgments. The author is very grateful for the sponsorship provided by the Fluid Dynamics Program (N00014-89-J-1100) and the Remote Sensing Program (N00014-89-J-3226), Office of Naval Research, and the Physical Oceanography Program (OCE-8716519), National Science Foundation.

REFERENCES

Banner, M. L., and E. H. Fooks, 1985: On the microwave reflectivity of small-scale breaking water waves. *Proc. Roy. Soc. London,* **A399,** 93–109.

——, I. S. F. Jones and J. C. Trinder, 1989: Wavenumber spectra of short gravity waves. *J. Fluid Mech.,* **198,** 321–344.

Daley, J. C., W. T. Davis and N. R. Mills, 1970: Radar sea return in high sea states. Rep. 7142, Naval Research Laboratory, Washington, D.C.

Donelan, M. A., and W. J. Pierson, Jr., 1987: Radar scattering and equilibrium ranges in wind-generated waves with application to scatterometry. *J. Geophys. Res.,* **92,** 4971–5029.

——, J. Hamilton and W. H. Hui, 1985: Direction spectra of wind generated waves. *Phil. Trans. Roy. Soc. London,* Ser. A, **315,** 509–562.

Duncan, J. R., W. C. Keller and J. W. Wright, 1974: Fetch and wind speed dependence of doppler spectra. *Radio Sci.,* **9,** 809–819.

Feindt, F., V. Wisman, W. Alpers and W. C. Keller, 1985: Airborne measurements of the ocean radar cross-section at 5.3 GHz. *Radio Sci.,* **21,** 845–856.

Fung, A. K. and K. K. Lee, 1982: A semi-empirical sea-spectrum model for scattering coefficient estimation. *I.E.E.E. J. Oceanic Eng.,* **OE-7,** 166–176.

Guinard, N. W., J. T. Ransone, Jr. and J. C. Daley, 1971: Variation of the NRCS of the sea with increasing roughness. *J. Geophys. Res.,* **76,** 1525–1538.

Hasselman, K., 1973: Measurements of wind–wave growth and swell decay during the Joint North Sea Wave Project (JONSWAP). *Hydrogr. Z.* (Suppl.), **A17,** 1–95.

Jessup, A. T., W. C. Keller and W. K. Melville, 1990: Measurements of sea spikes in microwave backscatter at moderate incidence. *J. Geophys. Res.,* in press.

Jones, W. L. and L. C. Schroeder, 1978: Radar backscatter from the ocean: dependence on surface friction velocity. *Bound.-Layer Meteor.,* **13,** 133–149.

Keller, W. C., W. J. Plant and D. E. Weissman, 1985: The dependence of X-band microwave sea return on atmospheric stability and sea state. *J. Geophys. Res.,* **90,** 1019–1029.

Kitaigorodskii, S. A., 1983: On the theory of the equilibrium range in the spectrum of wind generated gravity waves. *J. Phys. Oceanogr.,* **13,** 816–827.

Kwoh, D. S. W., B. M. Lake and H. Rungaldier, 1988: Microwave scattering from internal wave modulated surface waves: a shipboard real aperture coherent radar study in the Georgia Strait experiment. *J. Geophys. Res.,* **93,** 12 235–12 248.

Lee, P. H. Y., 1977: Doppler measurements of the effects of gravity waves on wind-generated ripples. *J. Fluid Mech.,* **81,** 225–240.

Liu, P. C., 1971: Normalized and equilibrium spectra of wind waves on Lake Michigan. *J. Phys. Oceanogr.,* **1,** 151–159.

Longuet-Higgins, M. S., 1969: On wave breaking and the equilibrium spectrum of wind-generated waves. *Proc. Roy. Soc. London,* **A310,** 150–159.

Masuko, H., K. Okamoto, M. Shimada and S. Niwa, 1986: Measurements of microwave backscattering signatures of the ocean surface using X band and Ka band airborne scatterometers. *J. Geophys. Res.,* **91,** 13 065–13 083.

Moore, R. K. and A. K. Fung, 1979: Radar determination of winds at sea. *Proc. I.E.E.E.,* **67,** 1504–1521.

Phillips, O. M., 1958: The equilibrium range in the spectrum of wind-generated ocean waves. *J. Fluid Mech.,* **4,** 426–434.

——, 1977: *The Dynamics of the Upper Ocean.* 2nd ed. Cambridge University Press,

——, 1985: Spectral and statistical properties of the equilibrium range in wind-generated gravity waves. *J. Fluid Mech.*, **156,** 505–531.

——, 1988: Radar returns from the sea surface—Bragg scattering and breaking waves. *J. Phys. Oceanogr.*, **18,** 1065–1074.

Schroeder, L. C., D. H. Boggs, G. Dome, I. M. Halberstam, W. L. Jones, W. J. Pierson and F. J. Wentz, 1982: The relationship between wind vector and normalized radar cross section used to derive SEASAT-A satellite scatterometer winds. *J. Geophys. Res.*, **87,** 3318–3336.

——, W. L. Jones, P. R. Schaffner and J. L. Mitchell, 1984: Flight measurements and analysis of AAFE RADSCAT wind speed signature of the ocean. NASA Tech. Memo. TM-85646,

Valenzuela, G. R., 1978: Theories for the interaction of electromagnetic and oceanic waves—a review. *Bound.-Layer Meteor.*, **13,** 61–85.

Wentz, F. J., S. Peteherych and L. A. Thomas, 1986: A model function for ocean radar cross sections at 14.6 GHz. *J. Geophys. Res.*, **89,** 3689–3694.

Woiceshyn, P. M., M. G. Wurtele, D. H. Boggs, L. F. McGoldrick and S. Peteherych, 1986: The necessity for a new parameterization of an empirical model for wind/ocean scatterometry. *J. Geophys. Res.*, **91,** 2273–2288.

Wu, Jin, 1980: Wind-stress coefficients over sea surface near neutral conditions—a revisit. *J. Phys. Oceanogr.*, **10,** 727–740.

——, 1988: Variations of whitecap coverage with wind stress and water temperature. *J. Phys. Oceanogr.*, **18,** 1448–1453.